

# Determination of Critical Delivery Head for Hydraulic Ram Pump

Philip Jun S. Celerinos<sup>1\*</sup> and Kristine D. Sanchez-Companion<sup>1, 2</sup>

<sup>1</sup>Graduate School of Engineering

<sup>2</sup>College of Engineering and Technology

Mindanao State University – Iligan Institute of Technology

Iligan City, 9200 Philippines

\*philipjun.celerinos@g.msuiit.edu.ph

Date received: May 5, 2021

Revision accepted: July 12, 2022

---

## Abstract

*In response to the continuous price increase of electricity and diesel fuel, a hydraulic ram pump serves as an alternative water pump that can be useful for farmers and low-income earning citizens living in mountainous areas. However, this pump was observed to have a critical delivery head to work uninterruptedly. This study conducted a field experiment of 10 design cases for drive pipe to determine the critical delivery head of the newly developed hydraulic ram pump using different pipe fittings and a 20-L disposable polycarbonate bottle as a pressure chamber. Results showed that the newly developed hydraulic ram pump reached its highest discharge efficiency of 12.83% and energy efficiency of 84.61% at 9.83 and 10.90 m critical delivery heads, respectively. Results also revealed that the critical delivery head was 86.27% linearly correlated with discharge efficiency and 46.78% linearly correlated with energy efficiency ( $p < 0.05$ ). Thus, the determination of the critical delivery head provided a baseline reference in ram pump studies that only gave ranges of ratios for the drive head to the delivery head. Furthermore, the newly developed hydraulic ram pump can produce water up to 700 L a day which can be beneficial for households and small-scale agricultural farming.*

**Keywords:** critical delivery head, delivery pipe, drive pipe, hydraulic ram pump

---

## 1. Introduction

As reported by the World Bank's Water Supply and Sanitation, around 7.5 million out of 94 million Filipinos still has no access to water supply facilities (Smets, 2015). Most of them are living in rural areas (World Health Organization, 2019). For instance, several remote areas in Mindanao are not within the service area of main water district providers, particularly in Bukidnon and Marawi City, wherein high-value crop production and the primary source of the hydroelectric power plant are located (Piñol, 2020).

These residents have been compelled to transport water from a source to their houses. A total of 7,460 water facilities were constructed in 2020, which covers places in Metro Manila, other highly urbanized cities, and geographically isolated and disadvantaged areas. However, about half of these facilities have minimal water supply capacities with unregulated water sources. One of the major issues includes difficulties in delivering materials for construction and maintenance, especially in those areas located in high altitude and remote villages (Department of the Interior and Local Government, 2021). Given the variability in water for their daily needs, these residents can draw water from any available source (e.g., rivers, lakes, or streams) using pumps powered by diesel fuel or electricity. However, getting fuel supply or electricity may pose a dilemma (Codera *et al.*, 2018) because of inaccessible site location and high inflation on these commodities (Lopez *et al.*, 2021). With the continuous price increase in fuel, generation charges at the Wholesale Electricity Spot Market (WESM) also increased. In effect, it provides high electric bills to residents (Lorenciana, 2021) and contributes to greenhouse gas emissions from carbon by-products generated from pumps mobility (Hennig and Haase, 2021).

To address the aforementioned issues, one alternative way to supply water to the residents living in these areas is to use an economical water pumping technology that does not use diesel fuel or electricity in the entire operation. This water pumping technology is called the hydraulic ram pump. It is a pumping device that allows rising water uphill without using any external power source (Hussin *et al.*, 2017). It only used the water hammer effect to develop pressure from the elevated source, which pushes a certain amount of water to higher elevations in a periodic operating cycle (Fatahi-Alkouhi and Lashkar-Ara, 2019). It has a simple water pumping system consisting of an elevated water source supply, drive pipe, ram pump body with two moving parts (i.e., waste valve and delivery valve), pressure chamber and delivery pipe (Sarma *et al.*, 2016; Hatipoğlu *et al.*, 2018; Asvapoositkul *et al.*, 2019). Recently, the necessity to use hydraulic ram pumps has been recognized to address renewable energy and sustainable technology needs (Kumar, 2022). Thus, the continuous development of this pump provides more interest to other researchers because of its contribution to rural communities and remote areas.

Owing to its simplicity and eco-friendly process, the hydraulic ram pump is most suitable in mountainous areas for farmers and low-income earning citizens with abundant water sources. In fact, this pump can be used for irrigation and domestic water supply (Sampath *et al.*, 2015). Recently,

Kesharwani *et al.* (2021) used a hydraulic ram pump for agricultural farming in a remote village in Taipadar, Central-East India. It has an 8-inch ram inlet and 4-inch ram outlet, manufactured by Rife Incorporated, using the river as the water source. They developed a ram scaling law that provides a criterion of head-discharge-diameter ratios. The predicted dimensionless characteristics of head ratios, discharge ratios and velocity ratios were identified as the governing parameters when optimizing large rams. Similarly, Li *et al.* (2020) identified the flow passage of head ratios as the main factor influencing the hydraulic ram pump performance. They created a novel waste valve that could decrease the head loss coefficient, optimize the delivery heads with relatively high efficiency and provide more water outputs. Hence, the head ratios were derived from establishing the design of the drive pipe and the delivery pipe. On the other hand, a small-scale hydraulic ram pump decreases back-head pressure due to the water hammer effect from the drive pipe length and its moving parts. The pressure shock in the delivery pipe was due to an increase in the air in the chamber, which resulted in a strong vibration of the drive pipe (de Carvalho *et al.*, 2016). These findings also agreed with Inthachot *et al.* (2015) wherein a small-scale hydraulic ram with a 1-inch ram inlet and 1/2-inch ram outlet was installed in the stream for irrigation in Northern Thailand. Aside from differing the check valves, varying the drive pipe lengths also influenced the water production because the actual setup of this pump is installed in different terrain elevations.

Previous literature for large-scale and small-scale rams pointed out that the drive and delivery pipes were among the parameters that must also be considered in designing an effective hydraulic ram pump. Analytically, the drive pipe length must be kept between four to 12 times the drive head (Maw and Htet, 2014). Moreover, Mondol (2017) suggested a range of design ratios of the drive pipe from elevated source supply to the ram pump placement from 1:3 to 1:7 head-to-distance ratio to produce a water hammer effect. On the other hand, the Permaculture Research Institute in Australia provided a conservative estimate of drive pipe to its delivery pipe head-to-head ratio of 1:7 so that the moving parts would uninterruptedly function in an open and close manner (Roberts, 2017). It also allows the delivery head to reach up to 12 times from the supply elevation (de Carvalho *et al.*, 2011). Existing studies and manufacturers only provide a range of values for the drive head to its delivery head ratios (Watt, 1974; Corps, 1981; Brown, 2006; Browne, 2009; Practical Action, 2010; de Carvalho *et al.*, 2011; Kumar, 2022; Jocags, 2017; Mondol, 2017; Roberts, 2017) as a reference in designing the water pumping system of the hydraulic ram pump.

The abovementioned studies only discussed the ranges of design ratios of head-to-head for the drive pipe and delivery pipe. The studies by de Carvalho *et al.* (2011), Mondol (2017) and Roberts (2017) did not emphasize the existence of the critical elevation for the delivery pipe in which the moving parts of the hydraulic ram pump could function uninterruptedly. Therefore, one needs to perform trial tests to be able to determine the critical delivery head, which can be tedious and time-consuming when constructing a water pumping system using a hydraulic ram pump. In general, no other related studies have emphasized the importance of determining the critical head of the delivery pipe in designing a functional and effective hydraulic ram pump.

This study aimed to determine the critical delivery head of the hydraulic ram pump from the varied drive pipe head-to-distance design ratios guidelines provided by Mondol (2017) and Roberts (2017). This study had specifically fourfold goals. First, it developed a small-scale hydraulic ram pump design using locally available pipe fittings with a 20-L disposable polycarbonate bottle as a pressure chamber. Second, it determined the critical delivery head of varied drive pipe head-to-distance design ratio in which the moving parts would function uninterruptedly. Third, the study verified the variables that influenced the obtained critical delivery head in which the experimental results allowed comparison through Bernoulli's energy principle. Finally, it established a relationship between the critical delivery head with discharge efficiency and energy efficiency variations.

## 2. Methodology

### 2.1 Design of Hydraulic Ram Pump

The newly developed hydraulic ram pump had a 730-mm width, 610-mm height, 25-mm inlet diameter and 12.5-mm outlet diameter (Figure 1b). The arrangement of each material was based on the hydraulic ram pump developed by Asvapoositkul *et al.* (2019). However, instead of using a 3-inch PVC tube as a pressure chamber, the authors utilized a 20-L disposable polycarbonate bottle found in any household. As stated by Junior *et al.* (2021), the ram pump performance can also be improved if the pressure chamber capacity is large enough for the compressed air to absorb and propagate pressure shock waves. Figure 1a shows the geometric configuration and working mechanism of the newly developed hydraulic ram pump as discussed by Kesharwani *et al.*

(2021). As illustrated, the formation of the water hammer when the waste valve was closed propagated a shock wave through the delivery valve that pushed an amount of water and repeated its cyclic operation. In the mentioned figure,  $Q$  is the discharge inflow from the source supply,  $q$  is the discharge outflow, and  $Q_{waste}$  is the excess water of the ram pump. The excess water served as the wastewater that cannot be delivered to the desired storage.

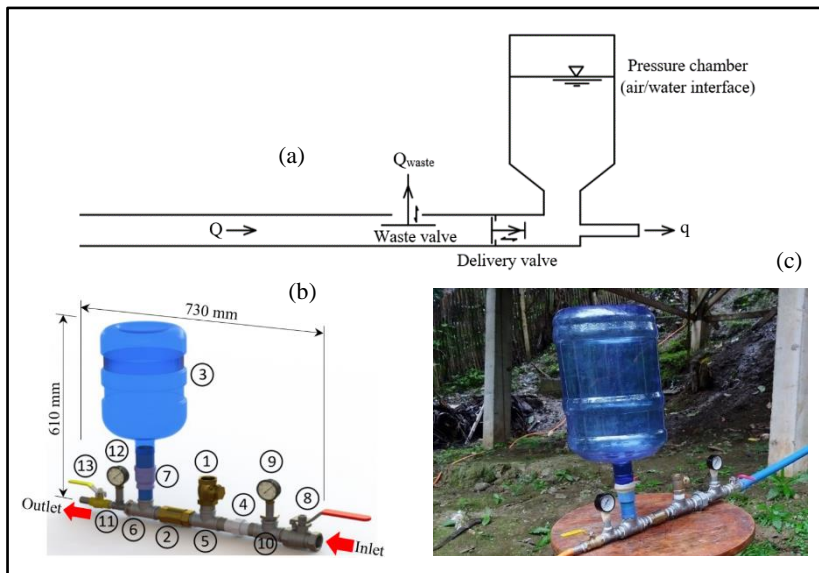


Figure 1. Newly developed hydraulic ram pump: geometric configuration and working mechanism (a), main components (b) and actual prototype (c)

The materials used in the newly developed hydraulic ram pump were composed of 12.5 to 25-mm diameter of galvanized iron (GI), brass, polyvinyl chloride (PVC) and stainless pipe fittings. The main components were the following (Figure 1b): (1) brass swing check valve, (2) brass spring check valve, (3) 20-L disposable polycarbonate bottle, (4) GI union fitting, (5, 6, 10, 11) stainless tee-fitting of different diameters, (7) PVC pipe, (8, 13) gate valve of different sizes and (9, 12) pressure gauge at inlet and outlet of the ram body. The actual product assembly of the newly developed hydraulic ram pump used in the field experiment is shown in Figure 1c, and the materials were bought from the local hardware store in Tagum City, Davao del Norte, Philippines.

## 2.2 Design System, Design Cases, Field Testing and Experimental Procedure

### 2.2.1 Water Pumping System

The design of the water pumping system (Figure 2) had three categorical parts: (1) elevated water source supply, (2) hydraulic ram body and (3) delivery. The experimental setup by Sarma *et al.* (2016), Hatipoğlu *et al.* (2018) and Asvapoositkul *et al.* (2019) was used as the reference for the water pumping system.

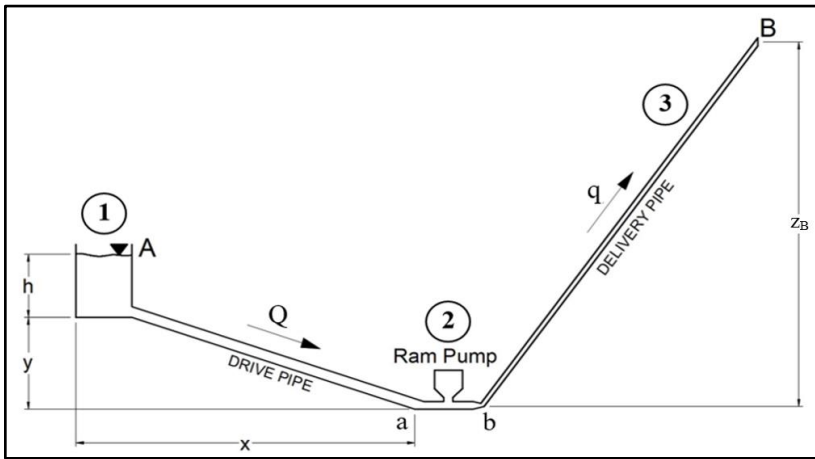


Figure 2. Schematic diagram of the water pumping system

In Figure 2, as discussed by Asvapoositkul *et al.* (2019), the cyclic operation started when the water tank at the elevated source discharged water down to the drive pipe. The drive pipe was elevated according to its head-to-distance design ratio. When the water entered the ram body at the inlet, the waste valve started to function and produced a water hammer effect. The delivery valve responded to the movement of the waste valve and generated pressure shock waves. Thus, an amount of water started to accelerate from the ram body outlet up to the delivery and the operation cycles continued.

Moreover, in Figure 2, the height of the water tank was  $h$  (m), the varied drive pipe elevation was  $y$  (m), while the varied drive pipe horizontal distance from supply elevation to the hydraulic ram pump was  $x$  (m). Also,  $A$  was the elevation level in which the water tank was full,  $z_B$  (m) was the elevation of the critical delivery head,  $B$  was the obtained level of the critical delivery head at which the moving parts started pumping without interruption,  $a$  was the ram

pump inlet and  $b$  was the ram pump outlet. The discharge inflow and discharge outflow were denoted as  $Q$  ( $\text{m}^3/\text{s}$ ) and  $q$  ( $\text{m}^3/\text{s}$ ), respectively.

2.2.2 Drive Pipe Head-to-Distance Ratio Design Cases

As highlighted by Kesharwani *et al.* (2021), Li *et al.* (2020), de Carvalho *et al.* (2016) and Inthachot *et al.* (2015), the drive pipe head-to-distance ratio is one parameter that must also be considered in hydraulic ram pump design. Hence, the length of the drive pipe is dependent on the source supply head (Mondol, 2017) because the hydraulic ram pump is installed from any water source (e.g., rivers, lakes, or streams) in different terrain elevations (Inthachot *et al.*, 2015). In this study, 10 design cases were considered using five varied heads and two head-to-distance ratios of the drive pipe (Mondol, 2017; Roberts, 2017).

In Table 1, the design cases were numbered from 1 to 10 based on the drive pipe head-to-distance ratio. The drive pipe heads were at 1.5, 1.8, 2.0, 2.3 and 2.5 m while the drive head-to-distance design ratios were 1:3 and 1:4.

Table 1. Data for drive pipe and delivery pipe used during the experiment

Design case no.	Drive pipe head (m)	Drive pipe distance (m)	Drive pipe diameter (mm)	Drive pipe length (m)	Drive pipe head-to-distance design ratio	Delivery pipe length (m)	Delivery pipe diameter (mm)
1	1.50	4.50	25	4.80	1:3	35	12.5
2	1.80	5.40	25	5.70	1:3	35	12.5
3	2.00	6.00	25	6.40	1:3	35	12.5
4	2.30	6.90	25	7.30	1:3	35	12.5
5	2.50	7.50	25	8.00	1:3	35	12.5
6	1.50	6.00	25	6.20	1:4	35	12.5
7	1.80	7.20	25	7.50	1:4	35	12.5
8	2.00	8.00	25	8.30	1:4	35	12.5
9	2.30	9.20	25	9.50	1:4	35	12.5
10	2.50	10.00	25	10.40	1:4	35	12.5

The drive pipe used a PVC pipe of different lengths for every design case. The drive pipe and delivery pipe diameter sizes were explained by Mondol (2017) that the typical pipe diameter of the delivery pipe is about half of the drive pipe diameter. On the other hand, the 35-m long delivery pipe used in each design case was based on the commercial availability of the flexible hose since Mondol (2017) likewise added that the length of the delivery pipe is much less critical than its head elevation.

Furthermore, the sizes of the pressure chamber, swing check valve and spring check valve are illustrated in Figure 1b. The authors did not provide a sniffer valve since the air in the pressure chamber using a 20-L disposable polycarbonate bottle produced pressure that was enough to pump water (Junior *et al.*, 2021).

### 2.2.3 Field Experiment Setup

The field experiment was performed in Brgy. Santo Niño, San Isidro, Davao del Norte, Philippines. It is situated in a remote highland area in the southeastern part of the Davao Region. The topographic view of the chosen site area is shown in Figure 3. It has a small river source wherein the water is drawn and used to supply the water pumping system. The field experiment was conducted consecutively for seven days (February 21-27, 2021). It had two separate daily testing operations: one was from 8:00 AM to 11:00 AM, while the other was from 1:00 PM to 4:00 PM.



Figure 3. Topographic view of the site area (Google, 2022)

Figure 4 shows the experimental setup based on the design of the water pumping system (Figure 2): (1) elevated water source supply, (2) hydraulic ram body and (3) delivery. The 200-L cylindrical plastic tank container was used in the field experiment as the source supply. The plastic tank had a height of 850 and 540-mm opening diameter. It was elevated according to the varied elevation of the drive pipe heads listed in Table 1.





Figure 4. Experiment setup of the water pumping system

#### 2.2.4 Determination of Critical Delivery Head and Other Measurements

A test trial was conducted prior to the actual experiment to determine the performance of the ram pump using varied drive head to delivery head ratios. This test trial paved way for a general observation that the ram pump could not immediately pump water and operate steadily. When the water pumping system started its cyclic operation, the moving parts of the hydraulic ram pump could not move on their own when the flexible hose was placed at different elevation levels for the delivery head. This phenomenon was not discussed in the literature (Mondol, 2017; Roberts, 2017) on which this current experimentation was based. Thus, the authors of the present work documented the observed phenomena. With this, the gate valve of the hydraulic ram pump's outlet was forced to close while the inlet gate valve was open. At this moment, the waste valve (swing check valve) was manually operated in an open and closed manner just to produce water. Consequently, the water slowly increased its level at the ram pump's pressure chamber until it occupied almost  $\frac{2}{3}$  of the volume in the 20-L disposable polycarbonate bottle. Thereafter, the outlet gate valve was slowly opened and the adjustments on the flexible hose were made to determine the exact location of the delivery head.

What was consistently observed was that there existed a critical level at which the moving parts would start to function. It was at this delivery head, termed the critical delivery head where the moving parts functioned uninterruptedly,

and the water was pumped continuously. When the critical delivery head was determined, a long tape measuring tool listed in Table 2 and the leveling equipment were used to measure the critical delivery head from the ram pump placement as a reference elevation in the water pumping system (Figure 2). Hence, the observed critical delivery head was consistent for the 10 different experimental setups (Table 1) and this procedure was applied in the same study area.

After the flexible hose was placed in their corresponding critical delivery heads, a five-minute observation period was allotted per design case before data recording. The following conditions were considered: (a) the number of beats of the swing check valve should have a uniform sound and variation; (b) the air volume in the pressure chamber should be constant in level; (c) the discharge inflow should be free from any debris since it may cause blockage in the delivery valve (spring check valve) movement; and (d) the water that goes out at the end of the critical delivery head should have a uniform discharge flow. These were all important in the water pumping system of the hydraulic ram pump so that the moving parts would continuously work until the water in the 200-L cylindrical plastic tank will be emptied.

After the allotted observation period and the critical delivery head was measured (m), the operation cycles of the water pumping system continued. At this moment, the data gathering was conducted. Tools and devices with uncertainty values used to measure the parameters during field testing are summarized in Table 2. The data gathering procedure was as follows: (a) the pressure at the gauge attached to the ram body outlet was recorded when the pointer of the pressure gauge pointed in the corresponding scale reading (kPa); (b) the depressed water level of the 200-L cylindrical plastic tank was measured by the caliper tool for a one-minute period using a stopwatch for the discharge inflow (L/min); (c) the water output at the critical delivery head was gathered for a minute using stopwatch and cylindrical plastic measuring beaker to determine the discharge outflow (L/min) and the waste water was then calculated (L/min); (d) the height level of the air at the pressure chamber using a 20-L disposable polycarbonate bottle was measured by the caliper tool to determine the volume interface between air and water (L); and (e) the number of beats of the swing check valve was counted for a minute using a stopwatch to determine the variation of sound behavior. Furthermore, a video was used to capture and record the determination of the critical delivery head.

Table 2. Details of measuring tools and devices used during field testing

Device/tool	Measured parameter*	Measuring range	Measuring accuracy
Pressure gauge	Ram pump outlet	0-150 psi	±0.25%
Stopwatch	Period of valve beat counts, water delivered and waste		0.01 s
Plastic beaker	Quantity of water delivered	1,000 mL	±0.01 mL
Cylindrical bucket	Quantity of wastewater	5 gal	
Caliper	Level of depressed water at discharge inflow and wastewater	0-150 mm	±0.01 mm
Long tape measure	Level of critical delivery head	0-100 ft	±0.001%

\*There were three initial trials for data measurements and were checked whether the initial data were closed to each other before proceeding to the actual data gathering.

### 2.3 Verification of Critical Delivery Head with Theoretical Delivery Head

Bansal (2010), Kudela (2012) and Subramanian (2014) stated that Bernoulli's equation provides an analysis that relates the elevation head, velocity head and pressure head of pumps. This equation also determines the head losses in pipes used. Hence, in this study, the critical delivery head obtained was compared with the theoretical delivery head.

To calculate the theoretical delivery head ( $z_B$ ), the energy equation between point  $b$  and point  $B$ , as illustrated in Figure 2, was established considering the friction loss in the delivery pipe. The equation used was from Bansal (2010) and Subramanian (2014) (Equation 1).

$$\frac{v_b^2}{2g} + \frac{p_b}{\gamma} + z_b - hf_{b-B} = \frac{v_B^2}{2g} + \frac{p_B}{\gamma} + z_B \quad (1)$$

where  $v_b$  is the velocity in the hydraulic ram pump outlet (m/s);  $p_b$  is the water pressure released in the hydraulic ram pump's outlet (kPa);  $z_b$  is the reference elevation of the water pumping system (m);  $hf_{b-B}$  is the pipe friction loss in the delivery pipe (m);  $v_B$  is the velocity of water in the delivery pipe end (m/s);  $p_B$  is the water pressure in the delivery pipe end (kPa);  $g$  is a constant gravitational acceleration ( $m/s^2$ ); and  $\gamma$  is the unit weight of water ( $kN/m^3$ ).

In this experiment, the velocity of water from the hydraulic ram pump's outlet up to the delivery pipe end was equal. In Equation 1, the expression of the velocity head  $\frac{v_b^2}{2g} = \frac{v_B^2}{2g}$  can be disregarded since there was no variation in the pipe diameter. Similarly, the pressure at the delivery pipe end was zero since the water was subjected to atmospheric pressure. Therefore, and taking in all these assumptions, Equation 1 can be simplified as:

$$\frac{P_b}{\gamma} - hf_{b-B} = z_B \quad (2)$$

Equation 2 indicates that the delivery head was dependent upon the pressure head at the outlet, which was point *b*, and the head loss due to friction in the delivery pipe. To calculate the friction factor in the delivery pipe ( $hf_{b-B}$ ), the derived major head loss using Darcy-Weisbach formula for the circular pipe (Kudela, 2012) was carried out upon establishing the energy equation between point *b* and point *B*, as shown in Figure 2. In Equation 3, the head loss due to pipe friction is given as:

$$hf_{b-B} = \frac{0.0826 f L Q^2}{D^5} \quad (3)$$

where *f* is the pipe friction factor; *L* is the length of the delivery pipe (m); *Q* is the discharge output (m<sup>3</sup>/s); and *D* is the diameter of the delivery pipe (mm).

To determine the pipe friction factor (*f*), Bansal (2010) specified that the water flow must be classified as either laminar or turbulent. The dimensionless value of the laminar flow must have a Reynolds number (*Re*) less than 2,000, while the latter must be greater than 3,000. Equations 4, 5 and 6 show the respective formulas.

$$Re = \frac{v D \rho}{\mu} \quad (4)$$

$$f_{Laminar} = \frac{64}{Re} \quad (5)$$

$$f_{Turbulent} = \frac{0.316}{Re^{0.25}} \quad (6)$$

where *v* is the velocity of water in the delivery pipe (m/s); *ρ* is the mass density of water (kg/m<sup>3</sup>); and *μ* is the water dynamic viscosity (Pa·s).

Furthermore, the performance of the hydraulic ram pump was determined by its obtained efficiencies output (Kesharwani *et al.*, 2021). These efficiencies were classified as the discharge output and energy.

The discharge efficiency ( $\eta_d$ ) is measured by its discharged output ( $q$ ) divided by the discharged input ( $Q$ ) (Mondol, 2017). If the discharge efficiency has a lower value, this indicates that the hydraulic ram pump has small water output considering the water input provided. In comparison, a bigger value indicates that the pump is efficient in providing discharge output. Equation 7 shows the hydraulic ram pump discharge efficiency.

$$\eta_d = \frac{q}{Q} \times 100\% \quad (7)$$

Lastly, Rankine's equation was used to evaluate the energy efficiency ( $\eta_e$ ) of the hydraulic ram pump as shown in Equation 8. The energy efficiency as specified by Mondol (2017) was measured by the discharged output ( $q$ ) times the critical delivery head ( $z_B$ ), divided by the discharged input ( $Q$ ) times the drive head ( $y$ ). This efficiency is a function of discharge output and head attained. If the energy efficiency has a lower value, this indicates that the hydraulic ram pump has provided a smaller discharge output considering water input and drive head in its critical delivery head attained; a bigger value provided a higher discharge output considering the water input and drive head in its critical delivery head attained.

$$\eta_e = \frac{qz_B}{Qy} \times 100\% \quad (8)$$

## 2.4 Statistical Analysis

The relationship among the critical delivery head, discharge efficiency and energy efficiency of the 10 varied design cases was determined through correlation and regression analysis. The Pearson correlation coefficient ( $r$ ), shown in Equation 9 and used by de Carvalho *et al.* (2016) and Fatahi-Alkouhi and Lashkar-Ara (2019) in their experimental study, was employed to measure the degree of relationship between variables considered. It also allows quantifying the strength of that relationship between variables and predicts the response values of the independent variable. Hence, the correlation coefficient was used to determine how strong a relationship was between the variables considered. To normalize the measurement of the covariance, the correlation coefficient result must be between -1 and +1. The value of +1 implied a strong

positive relationship between variables, while -1 indicated a strong negative relationship between variables. However, the correlation coefficient must be significantly non-zero value because, in this analysis, zero was defined as no correlation between variables (Walpole *et al.*, 2012).

Two hypotheses were formulated in the study. The first hypothesis (null hypothesis) stated that there was no linear correlation among the variables considered. The second hypothesis (alternative hypothesis) implied a linear correlation among the variables. A P-value with a 0.05 level of significance was set to select the acceptable hypothesis and the  $R^2$  rate was the parameter that verified the reported hypothesis value for the correlation and regression model. If the P-value is lesser than 0.05, the null hypothesis is accepted; otherwise, the alternative hypothesis is accepted. The equation is expressed as:

$$r = \frac{n \sum xy - (\sum x)(\sum y)}{\sqrt{[n \sum x^2 - (\sum x)^2][n \sum y^2 - (\sum y)^2]}} \quad (9)$$

where the critical delivery head is the independent variable  $x$ ; the discharge efficiency and the energy efficiency are dependent variables  $y$ ; and the 10 design cases considered as  $n$ .

### 3. Results and Discussion

#### 3.1 Hydraulic Ram Pump Performance

##### 3.1.1 Drive Head, Critical Delivery Head and Delivery Pipe Pressure

In Table 3, as observed in design cases 1 to 5 with a 1:3 drive pipe ratio and design cases 6 to 10 with a 1:4 drive pipe ratio, as the drive pipe head increased, the ram pump's outlet pressure increased. Likewise, as the drive pipe head increased, the obtained critical delivery head also increased. The lowest recorded outlet pressure was observed in design case 1 by 98 kPa with a 1.5-m drive pipe head at a 9.83 m critical delivery head. Also, the highest recorded outlet pressure was observed in design case 10 by 154 kPa with a 2.5-m drive pipe head at a 14.95-m critical delivery head. This record revealed that the newly developed hydraulic ram pump generated an increase in the

outlet pressure when the drive pipe head and the critical delivery head also increased. These results agreed with the previous findings of Sampath *et al.* (2015), who inferred that with the continued increase in the drive pipe head, the outlet pressure also increased. However, in addition to their obtained results, this study also provided findings on the relationship between the critical delivery head in the ram pump’s outlet pressure. Thus, an increase in the drive pipe head also resulted in an increase in both the outlet pressure and the critical delivery head (Table 3).

Table 3. Summary of data during the field experiment

Design case no.	Drive pipe head (m)	Critical delivery head (m)	Outlet pressure (kPa)	Discharge of water (L/min)			Vol. of water in pressure chamber (L)	Vol. of air in pressure chamber (L)	Beat counts per min
				Input	Output	Waste			
1	1.50	9.83	98	3.664	0.47	3.19	16.655	3.345	75
2	1.80	10.43	104	3.733	0.42	3.31	16.901	3.099	77
3	2.00	11.45	114	3.779	0.40	3.36	17.392	2.608	84
4	2.30	13.56	135	4.122	0.41	3.70	17.539	2.461	88
5	2.50	14.90	149	4.269	0.38	3.84	17.612	2.388	95
6	1.50	10.90	108	4.122	0.48	3.64	16.655	3.345	84
7	1.80	13.30	132	4.168	0.43	3.72	16.911	3.089	90
8	2.00	14.65	145	4.237	0.40	3.82	17.637	2.363	93
9	2.30	15.25	153	4.466	0.38	4.07	18.005	1.995	96
10	2.50	14.95	154	4.809	0.36	4.43	18.128	1.872	103

Table 4 shows the acquired ram pump’s outlet pressure head of the water pumping system from the calculation using Equation 2, which would be notable as the governing and dominating element in the critical delivery heads. The manual calculation results in Table 4 from the measured data in Table 3 confirmed that the increase in outlet pressure also increased the theoretical delivery head.

Additionally, as observed during the field experiment, longer drive pipe length resulted in a higher water hammer effect and vibration. This parameter affected the performance of the newly developed hydraulic ramp pump, thereby reducing the critical delivery head. Another reason was that increasing the drive pipe length increased its friction loss from the calculated results (Table 4).

Table 4. Summary of results for the verification of theoretical delivery head

Case no.	Drive Pipe Length (m)	Pressure head (m) outlet	Velocity (m/s)		Friction losses in pipe length ( $h_f$ )		Theoretical delivery head ( $z_B$ ) (m)
			Inlet	Outlet	Drive pipe (m)	Delivery pipe (m)	
1	4.80	9.989	0.124	0.063	0.00642	0.04686	9.943
2	5.70	10.601	0.126	0.057	0.00787	0.04187	10.560
3	6.40	11.621	0.128	0.054	0.00903	0.03988	11.581
4	7.30	13.761	0.139	0.056	0.01199	0.04088	13.721
5	8.00	15.189	0.143	0.052	0.01379	0.03789	15.151
6	6.20	11.009	0.139	0.065	0.01018	0.04786	10.961
7	7.50	13.456	0.142	0.058	0.01256	0.04287	13.413
8	8.30	14.781	0.143	0.054	0.01430	0.03988	14.741
9	9.50	15.596	0.151	0.052	0.01795	0.03789	15.558
10	10.40	15.698	0.163	0.049	0.02237	0.03589	15.662

Table 5 exhibits the comparison between the theoretical delivery head calculated using Equation 2 and the critical delivery head obtained from field experiment. The interactions between the critical delivery head and the theoretical delivery head were very similar and almost coincided with each other with minor differences.

Table 5. Theoretical delivery head versus critical delivery head

Design case no.	Theoretical delivery head (m)	Critical delivery head (m)	Difference (m)
1	9.943	9.83	(0.113)
2	10.560	10.43	(0.130)
3	11.58	11.45	(0.131)
4	13.721	13.56	(0.161)
5	15.151	14.90	(0.251)
6	10.961	10.90	(0.061)
7	13.413	13.30	(0.113)
8	14.741	14.65	(0.091)
9	15.558	15.25	(0.308)
10	15.662	14.95	(0.712)



Figures 5a and 5b also confirmed that as the drive head increased, the critical delivery head and theoretical delivery head also increased. Table 5 shows that design case 10 had the highest variance of 0.712 m as plotted in Figure 5b.

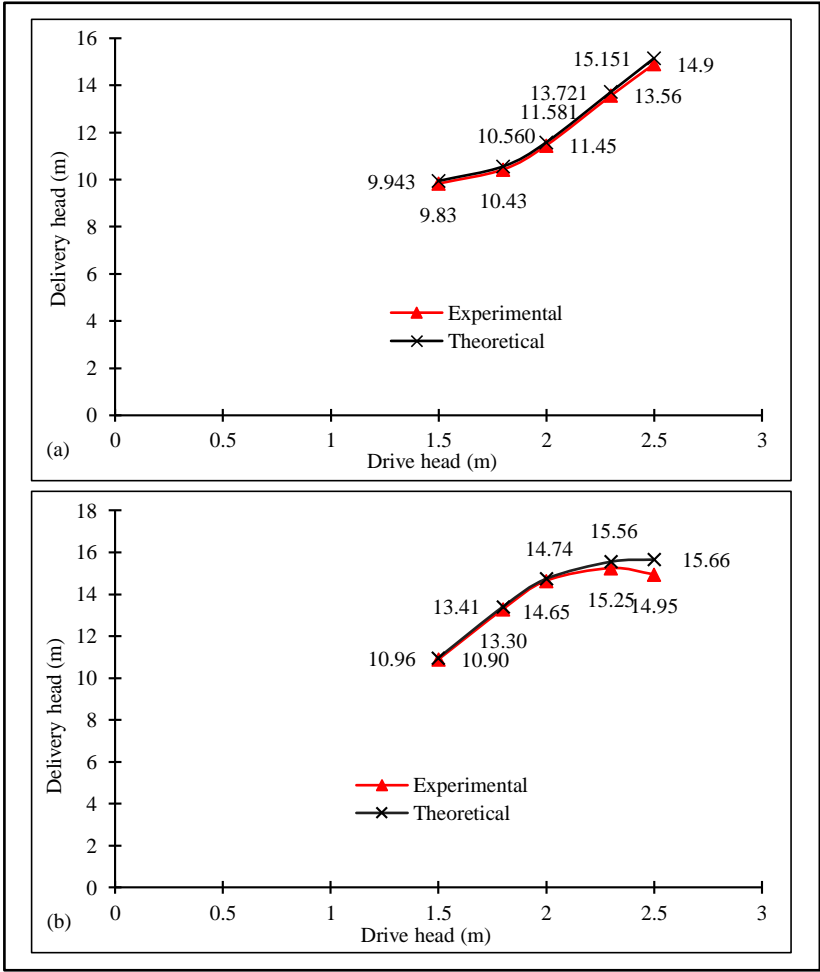


Figure 5. Drive head versus the critical delivery head and the theoretical delivery head using 1:3 (a) and 1:4 (b) ratios

This variance was due to some uncontrollable conditions during the field experiment and the contribution of pipe friction loss in the delivery pipe calculated using Equation 3 (Table 4). Moreover, the following conditions during the field experiment included: (a) slight water leaking at the drive pipe connections since the commercial length availability was only 3 m; (b) strong water hammer effect at moving parts which caused the longer drive pipe to

vibrate resulting into unstable water flow; and (c) wiggling alignment of the drive pipe length during operation due to strong vibration that affected the ram pump's performance. The conditions mentioned were also linked to the findings of Asvapoositkul *et al.* (2019), who highlighted that the longer drive pipe lengths affected the ram's pumping operation.

### 3.1.2 Waste Valve Beating Count

For higher values of the critical delivery head, the number of beats per minute of the swing check valve increased as observed in design cases 1 to 10 (Table 3). Each swing check valve beat corresponded to the water delivered and water spilled. An increase in waste valve stroke variations from 75 beats/min to 95 beats/min for 1:3 ratio and 84 beats/min to 103 beats/min for 1:4 ratio may increase the water spilled. This was because the swing check valve beating counts required a time period for its working cycle in close and open conditions. Apparently, the principle of the water hammer effect modified the sudden increase of pressure in the drive pipe and may result in an abruptly closed motion of the swing check valve with the corresponding spillage of water (Asvapoositkul *et al.*, 2019). This result showed a decreased water output when the swing check valve counts increased. A higher drive head resulted in greater energy of the water, but this entire energy cannot be fully extracted and some of it was delivered as water output; however, a portion of this water was wasted. In fact, the wasted water exiting from the waste valve was simply the energy of the water (Suraj *et al.*, 2018). Hence, an increase in the drive pipe head increased not only the critical delivery head but the waste water as well. The waste water increased was indicated by an increase in the number of beats in the swing check valve.

### 3.1.3 Pressure Chamber

Another observation during the field experiment was that the air volume in the pressure chamber decreased as the drive pipe length increased (Table 3) since compressed air started to dissolve. As observed between design cases 9 and 10, the critical delivery head reduced from 15.25 to 14.95 m, and the water volume in the pressure chamber continued expanding from 18.005 to 18.128 L. It was explained by de Carvalho *et al.* (2016), Hatipoğlu *et al.* (2018) and Junior *et al.*, (2021) that as the air inside the pressure chamber is compressed, the water continues to flow inside the ram body. The air in the pressure chamber absorbed the water hammer pressure during cyclic operation. As a result of the successive increase in drive pipe head and length, the compressed

air in the pressure chamber started to dissolve. In effect, more water became waste (Table 3). These findings were observed during experimentation that the strong vibration affected the actual performance of the newly developed hydraulic ram pump, and the obtained critical delivery head started to decrease. Thus, this caused a fluctuating trend on the critical delivery head, which was evident in design cases 9 and 10 (Figure 5b) with 0.308 and 0.712 m variance from the theoretical delivery head. Ergo, both design cases decreased the obtained critical delivery heads.

3.2 Working Efficiency

The working performance of the newly developed hydraulic ram pump was evaluated with two governing efficiency equations using Equations 7 and 8. Mondol (2017) mentioned that these efficiencies were classified by discharge efficiency and energy efficiency. Table 6 shows the discharge efficiency and energy efficiency of 10 design cases along with their corresponding critical delivery head.

Table 6. Discharge efficiency and energy efficiency at the critical delivery head

Design case no.	Critical delivery head (m)	Discharge efficiency (%)	Energy efficiency (%)
1	9.83	12.83	84.06
2	10.43	11.25	65.60
3	11.45	10.59	60.60
4	13.56	9.95	58.63
5	14.90	8.97	53.45
6	10.90	11.64	84.61
7	13.30	10.32	76.23
8	14.65	9.44	69.15
9	15.25	8.51	56.42
10	14.95	7.49	44.76

In Table 6, the highest calculated discharge efficiency using Equation 7 was 12.83% at the critical delivery head of 9.83 m for design case 1, while design case 10 had the lowest discharge efficiency of 7.49% at the critical delivery head of 14.95 m. However, in energy efficiency using Rankine’s equation (Equation 8), design case 6 had the highest value of 84.61% at the critical delivery head of 10.90 m. Similarly, design case 10 still had the lowest value of 44.76% at the critical delivery head of 14.95 m. Asvapoositkul *et al.* (2019) underscored that the increasing head, distance and length in the drive pipe also increase the velocity and momentum of water in the drive pipe. These caused more water spilled, increased waste valve beats, higher critical delivery head

and decreased efficiency outputs. Hence, in this study, a 25-mm diameter hydraulic ram pump with a shorter drive pipe head and length created less water pressure and less critical delivery head. This can be observed in design case 1, which provided a slower stroke rate at 75 beats/min with less water spilled and more water delivered at 12.83 and 84.06% discharge efficiency and energy efficiency, respectively.

On the other hand, those with longer drive pipe lengths consumed more water, which resulted in more waste water and less water output. As evidenced in design case 10, a faster exit stroke and more water spillage at 103 beats/min yielded 7.49% discharge efficiency and 44.76% energy efficiency. It was mentioned by Asvapoositkul *et al.* (2019) that the beat of the waste valve also corresponded to the water delivered and water spilled. In addition, the reduction in efficiency was also from the reduced opening of the waste valve and its increased movement (Li *et al.*, 2020).

Moreover, the newly developed hydraulic ram pump using design case 1 had bigger water output produced considering water input provided, while design case 10 had smaller water output produced considering water input provided. These observations had comparable findings to the work of Kesharwani *et al.* (2021), who predicted the discharge outflow given the drive pipe design ratio and discharge inflow using the developed absolute scale chart. It was found that the desired efficiency might not be achieved if rigid materials such as GI steel pipe for the drive pipe are not used because water hammer would be the predominating factor affecting the operation that caused the drive pipe to vibrate. Mondol (2017) explained that as much as possible, the materials must be rigid when providing a much longer drive pipe. Since the authors used PVC materials for the drive pipe, it was observed that the longer drive pipe was affected by the water hammer vibration because the mechanical properties of PVC were less rigid and deflected more than 80 times than GI steel (Dutta and Vaidya, 2003). In effect, the critical delivery head level started to decrease, as well as the discharge and energy efficiency.

It was also evident that as the drive pipe length increased, the energy efficiency decreased. Hence, the energy efficiencies of design cases 4, 5, 9 and 10 were below the minimum standard energy efficiency output of the guidelines provided by Mondol (2017) (Figure 6). Similarly, in the discharge efficiency, its efficiency output also decreased as the drive pipe length increased. It was also observed in design cases 4, 5, 8, 9 and 10 that the obtained discharge efficiency fell below the minimum level (Mondol, 2017). Thus, the design

cases mentioned using a 25-mm diameter drive pipe beyond 7-m long implied poor performance for the newly developed hydraulic ram pump. Asvapoositkul *et al.* (2019) specified that if the drive pipe head and length become longer, a high-water momentum occurs, and the drive pipe might become damaged because of a strong vibration developed from the water hammer effect. Thus, it was advised to increase the drive pipe diameter.

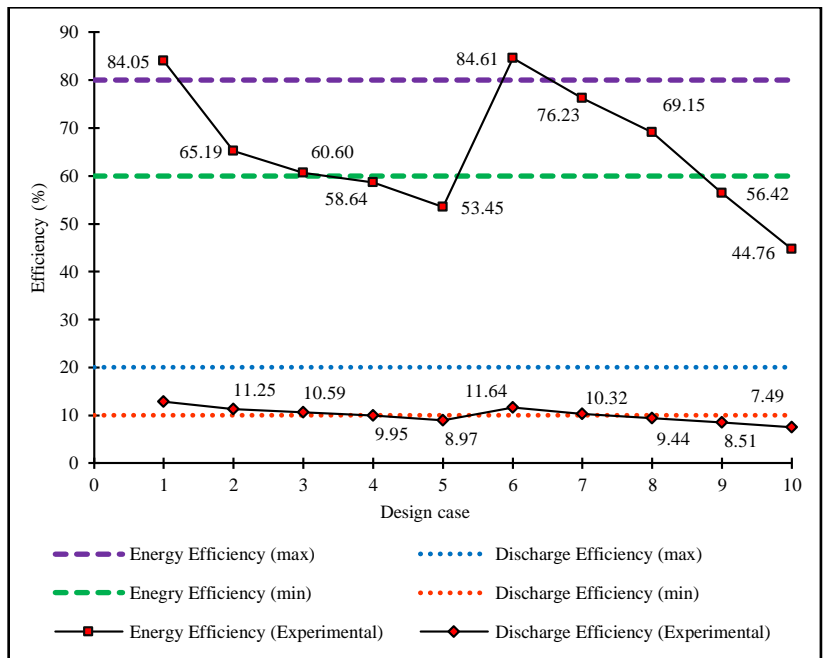


Figure 6. Efficiency outputs of the newly developed hydraulic ram pump

The hydraulic ram pump using design case 1 was the best design, which could pump 0.47 L/min of water at a 9.83-m critical delivery head with 12.83 and 84.06% discharge efficiency and energy efficiency, respectively. Eventually, if running water (e.g., rivers, lakes, or streams) is used as a source supply and if this water output is converted into daily water production, it can produce approximately 700 L of water a day. The approximated water output was based on the assumption that the ram pump operated for 24 h a day and had a constant supply of water. This quantity of water production can be helpful for households or for irrigation farming because around 40 to 80 L of water per day is needed to supply 100 to 200 plants for small-scale agricultural farming (Infonet-Biovision, 2010). In addition, Sampath *et al.* (2015) also stated that an average of 500 L of water usage is recommended for daily household purposes.

Furthermore, it is worthy to note that the fundamental method by other researchers was carried out in this study by plotting the head ratio against the discharge ratio (Schiller, 1986; Asvapoositkul *et al.*, 2019; Fatahi-Alkouhi and Lashkar-Ara, 2019) (Figure 7). The works of the mentioned authors used a constant drive pipe head; however, in this study, the drive pipe head values were varied. As shown below, for a 1:4 head-to-distance design ratio, an increasing head ratio resulted in an increase in the discharge ratio. This trend was not evident for the 1:3 head-to-distance design ratio, where the values plotted were scattered along the trend. It was clearly confirmed from the interpretation herein the curve diagram that the overall outcome of an increased discharge ratio versus the head ratio of the newly developed hydraulic ram pump was a reduction of its overall efficiency performance.

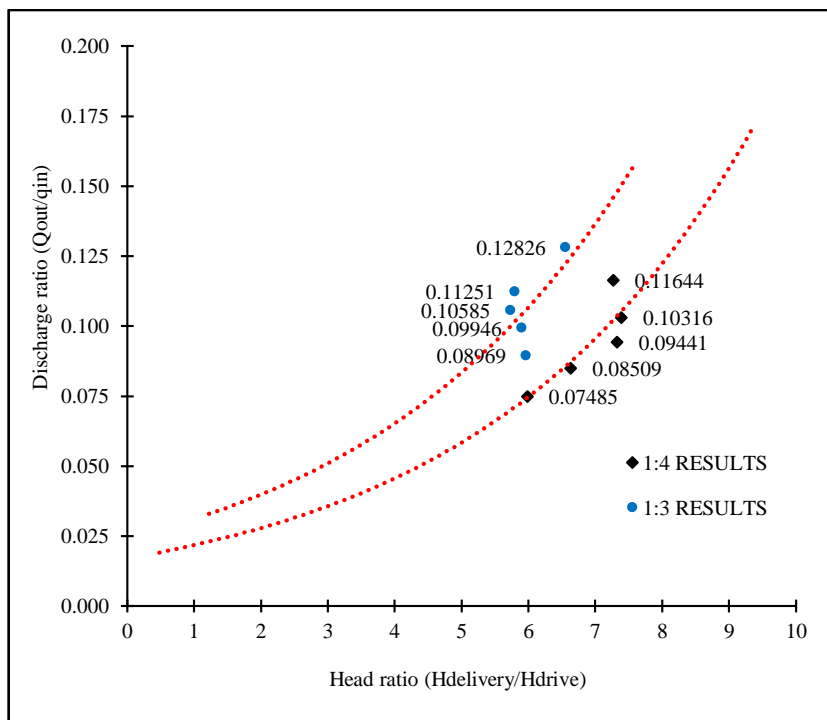


Figure 7. Characteristic curve of heads versus flow rates for 1:3 and 1:4 ratios

### 3.3 Relationship between Variation of Variables

The relationship between the critical delivery head with the discharge efficiency and energy efficiency output was investigated using correlation and regression analysis. The results confirmed that the critical delivery head was

linked to the discharge efficiency and energy efficiency relative to the design ratio of the 10 varied design cases (Table 7).

Table 7. Regression and correlation results of the critical delivery head with the two dependent variations

Variations	Level of significance ( $\alpha$ )	Selected hypothesis
Critical delivery head versus discharge efficiency	$r\text{-value} = -0.9288$ $R^2 = 0.8627$ $p = 0.0001$ $\alpha = 0.05$ $p < \alpha$	Reject the null hypothesis in favor of alternative hypothesis.
Critical delivery head versus energy efficiency	$r\text{-value} = -0.6839$ $R^2 = 0.4678$ $p = 0.0291$ $\alpha = 0.05$ $p < \alpha$	Reject the null hypothesis in favor of alternative hypothesis.

For the critical delivery head and the discharge efficiency variation, the computed P-value of 0.0001 was less than the set significance level (0.05). This result meant that the variables considered had linear relationships altogether. Thus, the null hypothesis between this variable was rejected in favor of the alternative hypothesis. The design cases revealed that the obtained critical delivery head provided a probable significant correlation coefficient  $R^2$  of 86.27% to the discharge efficiency output (Figure 8a). Since the correlation coefficient was in the range of 80 to 100%, this implied that the level of correlation was very strong. This analysis confirmed that as the critical delivery head increased, the discharge efficiency decreased. Hence, only 13.73% of the correlation was influenced by other factors.

Further investigations showed that the critical delivery head and the energy efficiency variation also had linear relationships. The formed null hypothesis was rejected in favor of the alternative hypothesis since the computed P-value of 0.0291 was less than the set significance level (0.05). Generally, the considered design cases revealed that the obtained critical delivery head provided a probable significant correlation coefficient  $R^2$  of 46.78% to the energy discharge efficiency output (Figure 8b). This result implied that the correlation between variables was moderately strong because  $R^2$  settled over the range of 40 to 59%. Thus, the correlation and regression analysis confirmed that the energy efficiency decreased when the critical delivery head increased. Hence, 53.22% was inclined towards the effects of other factors. This result may indicate that the obtained critical delivery head values did not strongly affect the energy efficiency.

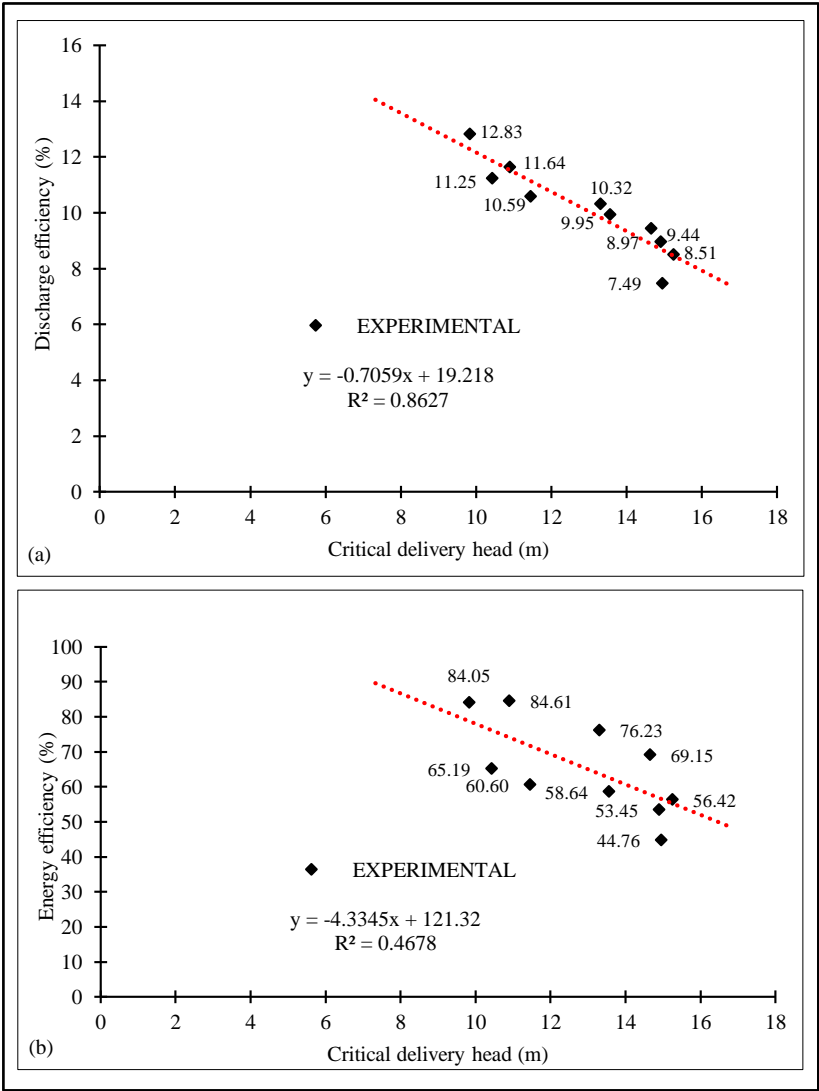


Figure 8. Critical delivery head versus discharge efficiency (a) and energy efficiency (b)

#### 4. Conclusion and Recommendation

The drive head and delivery head ratio provided by some manufacturers and mentioned in existing studies lack important emphasis and specifications



about the critical delivery head. Therefore, finding the critical delivery head before heading to the optimum delivery head is essential in the hydraulic ram pump design so that the moving parts could function continuously.

In this study, the critical delivery head was influenced by water pressure released in the ram pump's outlet from the generated pressure in the drive pipe head-to-distance design ratio, which formed a water hammer phenomenon through the moving parts. Higher water pressure was obtained by increasing the drive pipe head or reducing the drive pipe length which reduced friction loss. However, an increase in water pressure may result in higher waste water and an increase in the critical delivery head. This emphasized the importance of determining the critical delivery head that provided less waste water and higher discharge output.

The study also showed that the obtained critical delivery head significantly affected the hydraulic ram pump's efficiencies. Thus, when the critical delivery head became higher, the discharge efficiency and energy efficiency output decreased, which entailed poor performance of the hydraulic ram pump. Using 1:3 and 1:4 drive pipe head-to-distance ratios, the critical delivery head strongly correlated with the discharge efficiency but had a low correlation with the energy efficiency output. The newly developed hydraulic ram pump of this study required a drive pipe length between 4 to 7 m to provide adequate water output with higher energy efficiency achieved. This pump is a good alternative for the ones powered by electricity, diesel, or gasoline. It is useful for those residents living in highland areas since it can distribute water from the ram body placement to a minimum elevation of 9 m using 1:3 and 1:4 drive pipe head-to-distance ratios. The pump can continuously provide water up to 700 L a day using running water as the supply source. The materials used are accessible and mostly available in any hardware store with less maintenance cost.

## **5. Acknowledgement**

The main author is grateful for the help, support and guidance of his adviser and co-author, Dr. Kristine D. Sanchez-Companion. He would also like to recognize the Department of Science and Technology-Engineering Research and Development for Technology (DOST-ERDT) for the scholarship grant and research funding and the Graduate School of Engineering in Mindanao State University – Iligan Institute of Technology (MSU-IIT). Ultimately, he is

thankful for his wife (Ivanne Layka) and his two lovely daughters (Chrisvalle Alish and Christivanne Alish), who inspired him throughout the research.

## **6. References**

Asvapoositkul, W., Juruta, J., Tabtimhin, N., & Limpongsa, Y. (2019). Determination of hydraulic ram pump performance: Experimental results. *Advances in Civil Engineering*, 9702183. <https://doi.org/10.1155/2019/9702183>

Bansal, R.K. (2010). *Fluid mechanics and hydraulics machines* (9<sup>th</sup> ed.). New Delhi, India: Laxmi Publications Pvt. Ltd.

Brown, L. (2006). Using a hydraulic ram to pump livestock water. Retrieved from <https://lgpress.clemson.edu/publication/homemade-hydraulic-ram-pump-for-livestock-water/>

Browne, D. (2009). Design, sizing, construction and maintenance of gravity-fed system in rural areas. Retrieved from [https://www.pseau.org/outils/ouvrages/acf\\_gravity\\_fed\\_system\\_in\\_rural\\_areas\\_6\\_hydraulic\\_ram\\_pump\\_systems\\_2009.pdf](https://www.pseau.org/outils/ouvrages/acf_gravity_fed_system_in_rural_areas_6_hydraulic_ram_pump_systems_2009.pdf)

Codera, M.R., San Andres, L.G., Virrey, E.S., Leyda, J.M., Peña, J.C., & Sampot, V. H. (2018). Development of river current hydrokinetic siphoning device. *Proceedings of the 2018 IEEE 10<sup>th</sup> International Conference on Humanoid, Nanotechnology, Information Technology, Communication and Control, Environment and Management (HNICEM)*, Baguio City, Philippines, 1-5.

Corps, P. (1981). A training manual in conducting a workshop in the design, construction, operation, maintenance and repair of hydrams. Retrieved from <https://www.freessoft.org/hydram/hydram.pdf>

de Carvalho, M.O., Diniz, A.C.G.C., & Neves, F.J. (2011). Numerical model for a hydraulic ram pump. *International Review of Mechanical Engineering*, 5(4), 733-746.

de Carvalho, J.E.J., Saad, J.C.C., da Silva, N.I.F., Cunha, F.N., Teixeira, M.B., di Campos, M.S., & Barbosa, R.E.Z. (2016). Performance of a water ram built with disposable bottles. *African Journal of Agricultural Research*, 11(34), 3197-3202. <https://doi.org/10.5897/ajar2016.11107>

Department of the Interior and Local Government. (2021). A total of 7,460 projects have been completed under DILG's water supply and sanitation programs, giving 3.9 million households access to safe and sufficient water and sanitation. Retrieved from <https://dilg.gov.ph/news/A-total-of-7460-projects-have-been-completed-under-DILG-s-water-supply-and-sanitation-programs-giving-39-million-households-access-to-safe-and-sufficient-water-and-sanitation-/NC-2021-1056>

Dutta, P.K., & Vaidya, U. (2003). *A study of the long-term applications of vinyl sheet piles*. Mississippi, United States: Engineer Research and Development Center.

Fatahi-Alkouhi, R., & Lashkar-Ara, B. (2019). Experimental evaluation of effective parameters on characteristic curves of hydraulic rampumps. *Scientia Iranica*, 26(1), 283-294. <https://doi.org/10.24200/sci.2017.4597>

Google. (2020). Barangay Santo Niño, San Isidro, Davao del Norte satellite image. Retrieved from <https://earth.google.com>

Hatipoğlu, T., Nakay, İ., Köksal, E., & Fırlalı, A. (2018). Feasibility analysis of a hydraulic ram pump investment project. *Arabian Journal of Geosciences*, 11(9), 1-4. <https://doi.org/10.1007/s12517-018-3491-9>

Hennig, M., & Haase, M. (2021). Techno-economic analysis of hydrogen enhanced methanol to gasoline process from biomass-derived synthesis gas. *Fuel Processing Technology*, 216, 106776. <https://doi.org/10.1016/j.fuproc.2021.106776>

Hussin, N.S.M., Gamil, S.A., Amin, N.A. M., Safar, M.J.A., Majid, M.S.A., Kazim, M.N.F.M., & Nasir, N.F.M. (2017). Design and analysis of hydraulic ram water pumping system. *Journal of Physics: Conference Series*, 908(1), 012052. <https://doi.org/10.1088/1742-6596/908/1/012052>

Infonet-Biovision. (2010). Water for irrigation. Retrieved from <https://infonet-biovision.org/EnvironmentalHealth/Water-irrigation>

Inthachot, M., Saehaeng, S., Max, J.F., Müller, J., & Spreer, W. (2015). Hydraulic ram pumps for irrigation in Northern Thailand. *Agriculture and Agricultural Science Procedia*, 5, 107-114. <https://doi.org/10.1016/j.aaspro.2015.08.015>

Jocags. (2017). What is a ram pump and how it works? Retrieved from <https://gilmanrampump.com/aboutramppump/>

Junior, M.V.D.O., da Silva, R.T.L., Moreira, W.K.O., de Souza, J.L., Sarmento, C.S., & dos Santos Rodrigues, J.L. (2021). Performance of hydraulic ram built with different volumes of PVC air chambers. *Revista Engenharia na Agricultura-Reveng*, 29, 17-27. <https://doi.org/10.13083/reveng.v29i1.10900>

Kesharwani, S., Tripura, K., & Singh, P. (2021). Classical hydraulic ram pump performance in comparison with modern hydro-turbine pumps for low drive heads. *Proceedings of the Institution of Mechanical Engineers, Part A: Journal of Power and Energy*, 235(6), 1463-1486. <https://doi.org/10.1177/0957650921997202>

Kudela, H. (2012). Hydraulic losses in pipes. Retrieved from <http://www.energiazero.org/esercizi/hydraulic%20losses%20in%20pipes.pdf>

Kumar, H.D. (2022). Pollution free design and manufacturing of hydraulic ram pump for villages in hill areas. *International Research Journal of Modernization in Engineering Technology and Science*, 4(6), 782-796.

Li, J., Yang, K., Guo, X., Huang, W., Wang, T., Guo, Y., & Fu, H. (2020). Structural design and parameter optimization on a waste valve for hydraulic ram pumps. *Proceedings of the Institution of Mechanical Engineers, Part A: Journal of Power and Energy*, 235(4), 747-765. <https://doi.org/10.1177/0957650920967489>

Lopez, N.S., Tria, L.A., Tayo, L.A., Cruzate, R.J., Oppus, C., Cabacungan, P., Isla, I., Jr., Ansay, A., Garcia, T., Cabarrubias-Dela Cruz, K., & Biona, J.B.M. (2021). Societal cost-benefit analysis of electric vehicles in the Philippines with the inclusion of impacts to balance of payments. *Renewable and Sustainable Energy Reviews*, 150, 111492. <https://doi.org/10.1016/j.rser.2021.111492>

Lorenciana, C. (2021). Cebu's high power rates due to generation charge, others. Retrieved from <https://www.pna.gov.ph/articles/1139149>

Maw, Y.Y., & Htet, Z.M. (2014). Design of 15-meter head hydraulic ram pump. *International Journal of Scientific Engineering and Technology Research*, 3(10), 2177-2181.

Mondol, S.S. (2017). Design, manufacture and test a hydraulic ram (Thesis). Department of Mechanical Engineering, Heritage Institute of Technology, West Bengal, India.

Piñol, E. (2020). AIDFI ram pumps for Mindanao: Negros trip rediscovers 240-year old technology. Retrieved from <https://minda.gov.ph/news/482-aidfi-ram-pumps-for-mindanao-negros-trip-rediscovers-240-year-old-technology>

Practical Action. (2010). Hydraulic ram pumps. ITDG. Retrieved from [https://sswm.info/sites/default/files/reference\\_attachments/PRACTICAL%20ACTION%204000%20Hydraulic%20Ram%20Pumps.pdf](https://sswm.info/sites/default/files/reference_attachments/PRACTICAL%20ACTION%204000%20Hydraulic%20Ram%20Pumps.pdf)

Roberts, T. (2017). Hydraulic ram pumps. Retrieved from <https://www.permaculturenews.org/2017/09/18/-hydraulic-ram-pumps/>

Sampath, S.S., Shetty, S., Pendanathu, A.M., Javaid, W., & Selvan, M.C.P. (2015). Estimation of power and efficiency of hydraulic ram pump with re-circulation system. *International Journal of Computer-aided Mechanical Design and Implementation*, 1(1), 7-18. <http://dx.doi.org/10.14257/ijcmndi.2015.1.1.02>

Sarma, D., Das, M., Brahma, B., Pandwar, D., Rongphar, S., & Rahman, M. (2016). Investigation and parameter optimization of a hydraulic ram pump using Taguchi method. *Journal of the Institution of Engineers (India): Series C*, 97(4), 551-559. <https://doi.org/10.1007/s40032-016-0295-0>

Schiller, E.J. (1984). The hydraulic ram pump: Its history, operating characteristics, and potential usage. In E. J. Schiller (Ed.), *Proceedings of a Workshop on Hydraulic Ram Pump (Hydrant) Technology*, Arusha, Tanzania, 11-23.

Smets, S. (2015). Water supply and sanitation in the Philippines: Turning finance into services for the future. Retrieved from <http://documents.worldbank.org/curated/en/469111467986375600/pdf/100894-WSP-P131116-AUTHOR-Susanna-Smets-Box393244B-PUBLIC-WSP-SERIES-WSP-Philippines-WSS-Turning-Finance-into-Service-for-the-Future.pdf>

Subramanian, R.S. (2014). Engineering Bernoulli equation. Retrieved from <https://lin-web.clarkson.edu/projects/subramanian/ch330/notes/Engineering%20Bernoulli%20Equation.pdf>

Suraj, N., Pranav, P.S., Purusothaman, D., & Sivasankar, V. (2018). Design and fabrication of a hydraulic ram pump. *International Journal of Engineering Research and Technology*, 6(4), 1-4.

Walpole, R.E., Myers, R. H., Myers, S.L., & Ye, K. (2012). *Probability and statistics for engineers and scientists* (9<sup>th</sup> ed.). London, United Kingdom: Pearson Education, Inc.

Watt, S.B. (1974). A manual of information on the automatic hydraulic ram for pumping water. intermediate technology development group, water development unit. Retrieved from: <https://www.ircwash.org/sites/default/files/232.5-74MA.pdf>

World Health Organization. (2019). Water shortage in the Philippines threatens sustainable development and health. Retrieved from <https://www.who.int/philippines/news/feature-stories/detail/water-shortage-in-the-philippines-threatens-sustainable-development-and-health>